

## Supplementary Information for:

### High-Performance Mid-Infrared Linear Polarizers Using Fabry-Pérot-Resonant HSQ-based Gratings via a Simplified Fabrication

Xiaojia Liang<sup>1,2,3,4,†</sup>, Jingyuan Zhu<sup>1,2,3,4,†</sup>, Qing Zhong<sup>6,†</sup>, Chao Feng<sup>1,2,3,4</sup>, Siyu Dong<sup>1,2,3,4,\*</sup>, Zeyong Wei<sup>1,2,3,4</sup>, Hongfei Jiao<sup>1,2,3,4</sup>, Zhanshan Wang<sup>1,2,3,4,5</sup>, Xinbin Cheng<sup>1,2,3,4,5,\*</sup>

<sup>1</sup>Institute of Precision Optical Engineering, School of Physics Science and Engineering, Tongji University, Shanghai 200092, China.

<sup>2</sup>MOE Key Laboratory of Advanced Micro-Structured Materials, Shanghai 200092, China.

<sup>3</sup>Shanghai Frontiers Science Center of Digital Optics, Shanghai 200092, China.

<sup>4</sup>Shanghai Professional Technical Service Platform for Full-Spectrum and High-Performance Optical Thin Film Devices and Applications, Shanghai 200092, China.

<sup>5</sup>Shanghai Institute of Intelligent Science and Technology, Tongji University, Shanghai 200092, China.

<sup>6</sup>Graduate School of China Academy of Engineering Physics, Mianyang 621000, China.

\*Corresponding author: dongsy@tongji.edu.cn (Siyu Dong); chengxb@tongji.edu.cn (Xinbin Cheng).

†These authors contributed equally to this work.

Note 1: Influence of metal grating substrate and metal on TM transmission

We used RCWA to calculate the TM transmission of a 350 nm-period grating with a duty cycle of 0.5 and a metal thickness of 400 nm. Figure S1(a) shows that TM transmission changes a lot with substrate index. A higher substrate index gives lower TM transmission. Figure S1(b) shows that changing the metal causes only small differences. These results prove that the substrate is the main source of Fresnel loss. Besides, Low-index substrates for the mid-infrared are limited. Common options such as  $\text{CaF}_2$  and  $\text{ZnS}$  have several drawbacks compared with silicon. They have poor mechanical strength, are sensitive to moisture, and are more expensive. More importantly, because they are insulating, electron-beam lithography for fine gratings is also more difficult on these substrates. Moreover, changing the substrate can raise the TM transmission, but metallic gratings still cannot match our bilayer design while keeping a large extinction ratio. Even with a low-index  $\text{CaF}_2$  substrate, the average TM transmission is about 86.1%, which is lower than the 94% of our bilayer gratings.

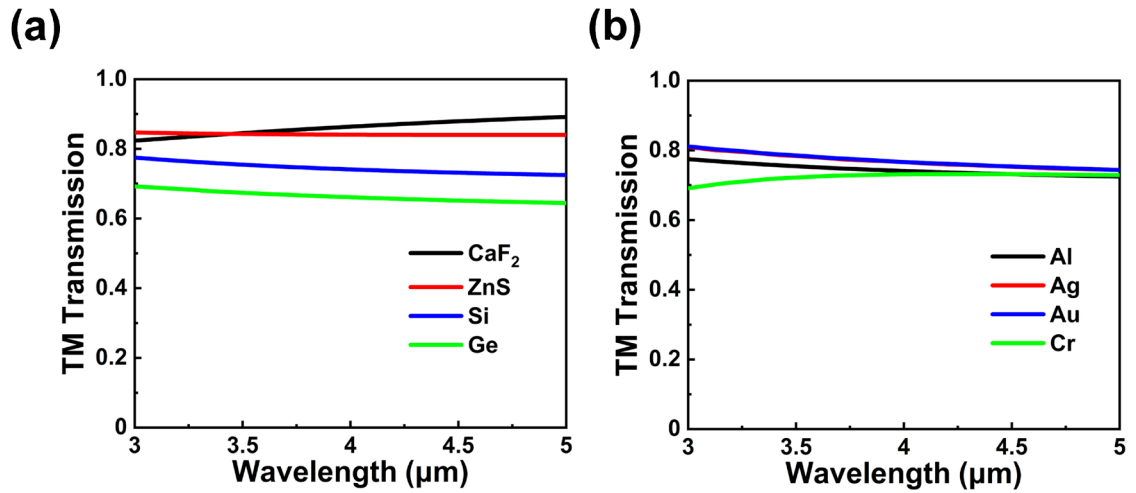


**Figure. S1** Simulated TM transmission for (a) different MIR-transparent substrates and (b) different metals.

## Note 2: Influence of Spacer Refractive Index and Thickness on the Optical Performance of the Bilayer Gratings

To evaluate how other dielectric spacers influence the optical response, we performed additional simulations in which the spacer refractive index and thickness were varied systematically. The new results are presented in Figure S2. In our analysis we define the bandwidth as the wavelength range where the TM transmission exceeds 90 %.

Figure S2(a-c) show the TM transmission, extinction ratio, extracted resonance wavelength and peak TM transmission as the spacer refractive index varies from 1.3 to 2 while keeping the thickness fixed at 230 nm. As the spacer index increases, the extinction ratio decreases monotonically. The resonance wavelength first decreases with increasing index, reaches a minimum near  $n \approx 1.75$ , and then rises again, whereas the peak TM transmission follows the opposite trend, increasing to a maximum at  $n \approx 1.75$  before slowly declining. The bandwidth remains constant across the refractive index range of 1.3-2. These results confirm that the device concept is compatible with a range of low-index spacers.

Figure 4(d-f) illustrates how varying the spacer-layer thickness from 0.18  $\mu\text{m}$  to 0.28  $\mu\text{m}$  at a fixed refractive index of 1.4 affects the polarizer's optical performance. The bandwidth increases with thickness at first and then remains constant beyond 0.21  $\mu\text{m}$ , consistently covering the 3–5  $\mu\text{m}$  range. The extinction ratio rises steadily as the thickness increases. The resonance wavelength shows the same upward trend. In contrast, the TM peak transmission decreases slightly as the thickness grows. Overall, the polarizer's optical properties show little sensitivity to spacer thickness variations.

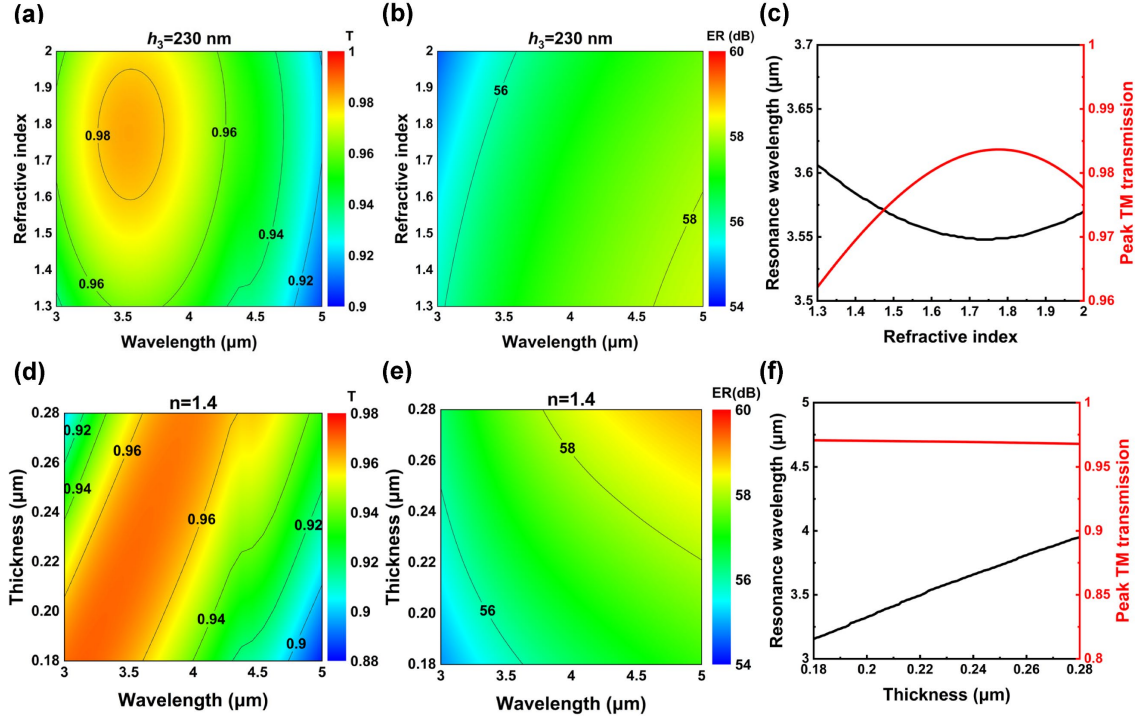


**Figure. S2** Simulated (a) TM transmission and (b) extinction ratio versus spacer refractive index. (c) Simulated resonance wavelength (black) and peak TM transmission (red) versus spacer refractive index. (d) TM transmission and (e) extinction ratio versus spacer thickness. (f) Resonance wavelength (black) and peak TM transmission (red) versus spacer thickness.

### Note 3: Effect of Grating Sidewall Slope on the Optical Performance of the Bilayer Gratings

We define the ratio of the top linewidth ( $L_t$ ) to the bottom linewidth ( $L_b$ ) as LR, which serves as an indicator of sidewall slope. Specifically, we modeled the HSQ grating as a trapezoid and assumed collimated metal deposition, as shown in Figure S3(a). We then performed FDTD simulations to sweep LR and obtained the corresponding TM transmission and extinction ratio. As shown in Figure S3 (b) and (c), the TM transmission and extinction ratio drop sharply when LR falls below 0.8, which corresponds to a sidewall angle of  $87.2^\circ$ . This confirms that, even with collimated metal deposition, a non-vertical sidewall significantly degrades the polarizer performance.

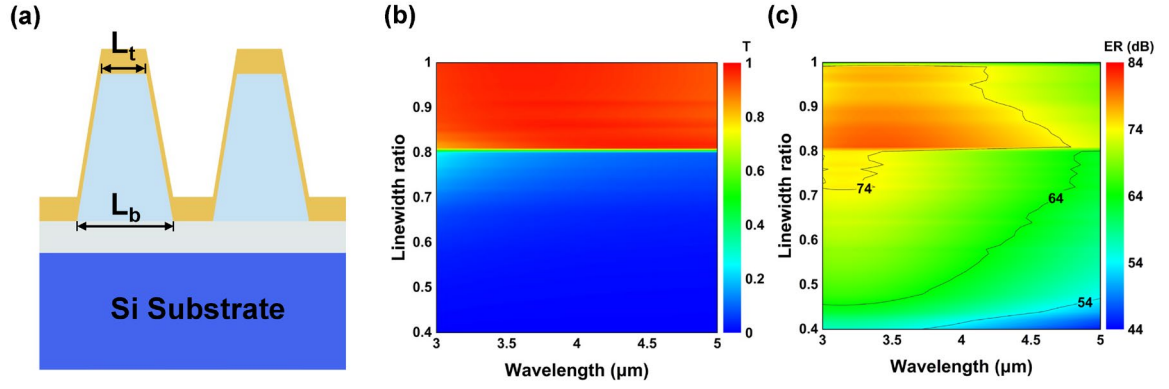


**Figure. S3** (a) Schematic of gratings as trapezoidal cross section. Simulated (b) TM transmission and (c) extinction ratio characteristics as a function of linewidth ratio.

Note 4: Spectra of bare Si, SiO<sub>2</sub>/Si, and the complete grating stack

Figure S4 shows modeled and measured spectra for three samples: bare Si, SiO<sub>2</sub>/Si, and the complete grating stack. The measured and simulated spectra of bare Si match well. For SiO<sub>2</sub>/Si and the full grating stack, small differences appear between simulation and experiment. These differences likely come from slight variations between the real refractive indices of the deposited films and the values used in the model. The spectra show that the SiO<sub>2</sub> layer works as an antireflection coating and increases the transmission by about 10% compared with bare Si. Adding the grating gives another increase of about 10%, so the average TM transmission reaches about 94%. This stepwise rise confirms that the high transmission of the full stack results from a Fabry–Perot–like resonance.

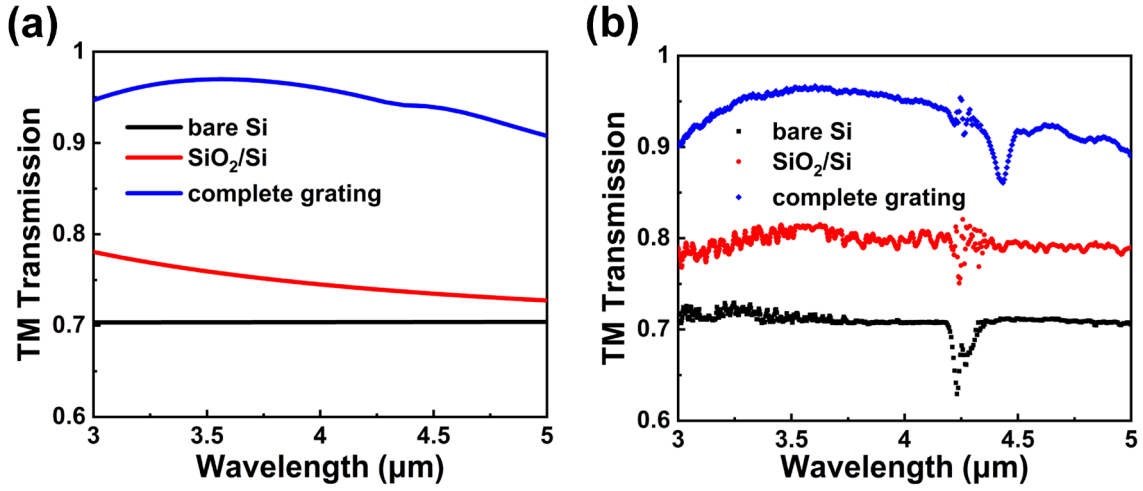


**Figure. S4** (a) modeled and (b) measured spectra for bare Si, SiO<sub>2</sub>/Si and the complete grating stack.

**Note 5: Thickness loss of HSQ layer during development**

The initial spin-coated thickness of the HSQ layer was indeed 400 nm. However, during the development process, partial dissolution of HSQ occurs, leading to a reduction in thickness. Under our development conditions (45 °C for 4 minutes), the HSQ thickness decreased to approximately 350 nm. As shown in Figure S5, simulation results demonstrate that the TM transmission and extinction ratio are very similar for HSQ thicknesses of 350 nm and 400 nm. Therefore, we did not strictly control the final HSQ thickness to remain exactly at 400 nm.

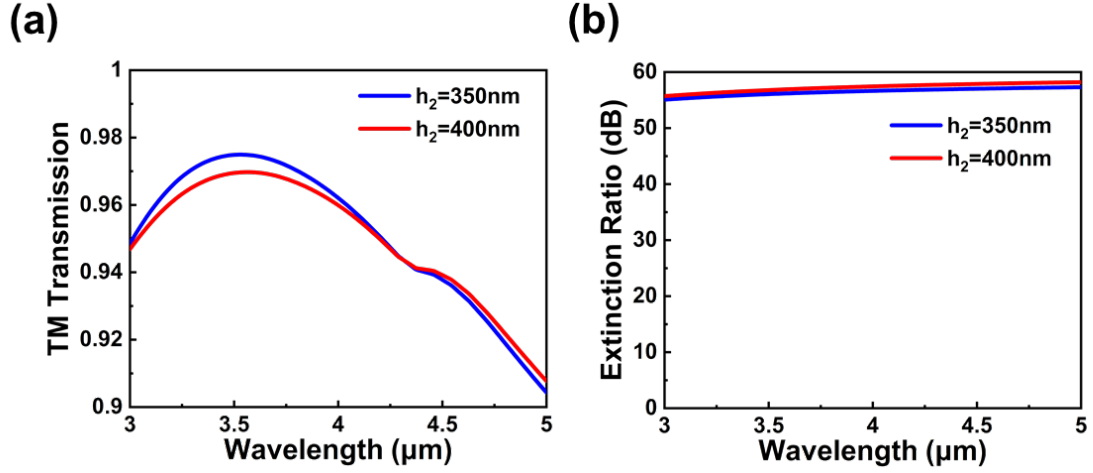
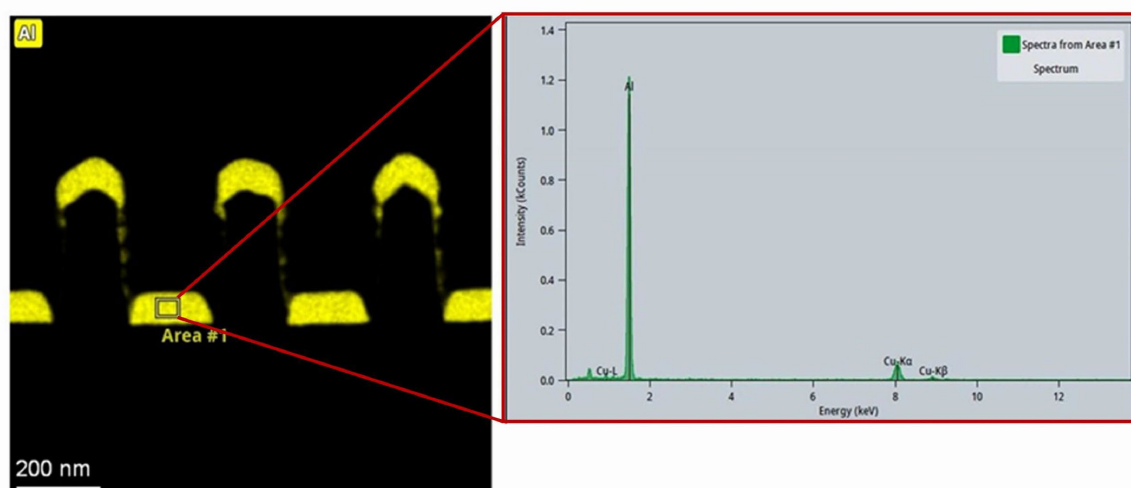


Figure. S5 Simulated (a) TM transmission and (b) extinction ratio for  $h_2 = 350\text{nm}$  (blue curve) and  $h_2 = 400\text{nm}$  (red curve) respectively.

#### Note 6: Details about EDX mapping

The EDX mapping was carried out by Materials Analysis Technology Inc. The specimens were prepared using Helios focused ion beam (FIB) system, and the subsequent EDX mapping was performed on a Talos transmission electron microscope (TEM). Figure S6 displays representative EDX spectrum acquired from the aluminum-rich region shown in Figure 5(b). The characteristic peaks corresponding to the Al K-edge are clearly visible, confirming the presence of aluminum in the measured area.



**Figure. S6** EDX spectrum of the aluminum-rich region in Figure 5(b).